

# STUDENTSKÁ PŘEHLÍDKA

## K POČÁTKŮM RENTGENOVÉ STRUKTURNÍ ANALÝZY V ČESKÝCH ZEMÍCH (DO R. 1945)

Emilie Těšínská

Archív AV ČR, V Zámčích 56/76, 181 00 Praha 8

Základy k využití Röntgenových paprsků X, objevených v r. 1895, ke studiu struktury hmoty byly položeny v r. 1912 a následujících pracemi M. v. Laueho, W. Friedricha a P. Knippinga, W. H. a W. L. Braggů, J. V. Wulfa a dalších. V Dodatcích k Ottově slovníku naučnému nové doby (Praha 1935) jsou tyto práce s retrospektivou následujících zhruba dvou desítek let charakterizovány slovy: “R. 1912 zasáhl náhle a mocně do rozvoje krystalografie objev, který rázem přiblížil k experimentálnímu řešení problém mřížoví krystalového, o němž byly možné dotud jen teoretické úvahy: von Laue objevil úkazy při průchodu Roentgenových paprsků krystaly, uživ krystalového mřížoví jako prostorové mřížky optické. Další roentgenometrické metody zavedené oběma Braggy, Debyem a Scherrerem umožnily stanovit kvantitativním měřením rozměry krystalového mřížoví a umístění jednotlivých atomů v něm. Za dvacet let následujících po objevu Laueho ... byla prozkoumána největší část krystalových hmot přirozených i umělých a důsledky tohoto prozkoumání atomové stavby prvků i sloučenin se jeví netušenými pokroky ve směru fyzikálně chemickém, geochemickém i prohloubení a experimentálním doložení názorů o isomorfii a ostatních vztazích krystalochemických.”...

Na počátku rozvoje rentgenové strukturní analýzy u nás stála **percepce** zmíněných zahraničních prací a objevů: na stránkách *Časopisu pro pěstování matematiky a fyziky* jsem první zmínku o pokusech Laueho a spol. s interferencí rentgenových paprsků na krystalech objevila v 42. ročníku (1913), v anotaci Dr. Josefa Štěpánka (datováno duben 1913) na knihu “Pohl, R: Die Physik der Röntgenstrahlen (Brunšvik 1912)”. V následujícím, 45. ročníku *Časopisu*, vyšel v r. 1915, byl pak publikován 36stránkový referát A. Hlaváčka “Spektrální rozbor Roentgenových paprsků”, pojednávající velmi podrobně o Laueho myšlence využít pro interferenci rentgenových paprsků atomové mřížky přirozených krystalů, o jejím experimentálním provedení Friedrichem a Knippingem, o teorii jevu a metodách vypracovaných postupně Laue, Braggy, Wulfem, a dalšími. O pracích Laueho a spol. a Braggů z r. 1912 bylo krátce referováno rovněž profesorem teoretické fyziky pražské české univerzity Františkem Závíškou v tzv. *Přehledech pokroků fyziky v letech 1911 a 1912*, v jím zpracované partii “Vedení elektřiny v plynech a radioaktivita”, v oddíle 2: “Paprsky Roentgenovy”, která vyšla tiskem v říjnu 1915. Příslib podrobnějšího referátu v následujícím ročníku *Přehledů* zůstal nenaplněn, neboť tento grandiózní projekt referátů o nejnovějších pracích ve fyzice, zahájený v r. 1901, zanikl. Zmínky o Laueově objevu a jeho významu pro studium hmoty lze nalézt na několika místech také např. v populárně vědeckém spisku docenta fyziky na české technice Julia Suchého “*Moderní názory o*

*podstatě elektřiny a hmoty*” (Praha 1917, nákladem vlastním).

Referáty o výše zmíněných pracích a objevech iniciovaly laboratorní pokusy a výzkumy: již na V. sjezdu českých přírodopytčů a lékařů, který se konal ve dnech 29.5.-3.6. 1914, tj. v předvečer vypuknutí první světové války, referoval v I. sekci věnované fyzice, matematice a astronomii, v její 4. schůzi dne 2. června, Al. Hlaváček “*O spektru paprsků Roentgenových*”. V resumé tohoto referátu otištěném ve sjezdovém *Věstníku* se uvádí: “*Referuje o ohybových zjevech na krystalech (Laue, Friedrich, Knipping), teorii prostorové mřížky, o pokusech Teradových dokazujících nehmotnost záření tyto zjevy způsobujících, o pokusech Braggů, Moseleye a Darwina, odkrývajících také homogenní záření, dále o spektrografech Broglieho s otáčejícím se krystalem a o spektrografu slidovém; o průchodu R.. Paprsků kovovými foliemi a užití pro difrakční spektrum. Uvádí souvislost vnitřních dějů hmoty s těmito zjevy (zejm. vliv tepelných kmitů ve hmotě) a oznamuje, že souvislost těchto ohybových zjevů se změnami struktury hmoty počal společně s Dr. P. Růžkem experimentálně sledovati na určitých případech.*”

První světová válka vnesla zdržení do rozvoje oboru nejen u nás. Průkopníkem rentgenometrie krystalů se u nás po první světové válce, po návratu z bojiště, stal krystalograf a mineralog. Bohuslav Ježek (1877-1950). První lauegramy jím byly údajně získány ve spolupráci s fyzikem Karlem Teigem v Ústavu teoretické fyziky při české univerzitě v Praze, v jehož čele stál F. Závíška.

K. Teige a B. Ježek pak také jako první zařadili tematiku rentgenometrie krystalů do výuky na přírodovědecké fakultě české univerzity: v zimním semestru 1922/23 vypsal Ježek přednášku “*Souměrnost a röntgenometrie krystalů*” (1 hodina týdně, v mineralogickém ústavu). Impulsem k tomu mu mohla být i přednáška “*O paprscích Röntgenových*” (2 h.) vypsaná prof. Závíškou v LS 1914. V následujícím školním roce 1923/24, v zimním semestru, byla vypsána jednak Teigem fyzikální přednáška “*Atomová teorie krystalových mřížoví*” (2 h.), jednak Ježekem znovu “*Röntgenografie krystalů*” (1) a navíc “*Samostatné práce röntgenografické*” (celkem 6 h. a jen pro omezený počet účastníků). Od letního semestru 1923/24 bylo pak “*Cvičení röntgenografické a röntgenometrické*” nadále vypisováno Ježkem a Teigem společně (v rozsahu 3 h.) a konalo se v Ústavu pro teoretickou fyziku. Ve šk. r. 1928/29 převzal za Ježka přednášky a praktická cvičení v rentgenometrii krystalů František Ulrich, který také zorganizoval v mineralogickém ústavu české univerzity moderně vybavenou laboratoř pro rentgenometrii krystalů.

V dobových českých vysokoškolských učebnicích fyziky zahrnuje partii o základech rentgenové strukturní



analýzy např. kniha profesora české techniky v Brně Vladimíra Nováka "*Fysika. Základní poznatky fyzikální na podkladě pokusném. (Pro posluchače vysokých škol, učitele a přátele věd přírodních.)*" (2. Druhé, změněné a doplněné, vydání, II. díl: Magnetismus a elektřina. Nauka o zářivé energii, Praha 1921)".

V návaznosti na proniknutí do laboratoří vysokoškolských ústavů a do vysokoškolské výuky vstoupila problematika rentgenové strukturní analýzy i mezi témata doktorských disertačních prací: v názvech disertačních prací podaných na pražské české univerzitě se poprvé explicitně objevuje pojem rentgenových paprsků ve šk. r. 1916/17, v disertaci Rudolfa Šimůnka (nar. 1892), nazvané "*Interference Roentgenových paprsků*". Posouzení této disertace bylo přiděleno profesorům F. Závíškovi a B. Kučerovi.

K prvním českým monografiím v oboru výzkumu a aplikací rentgenových paprsků, vydaným do r. 1945, patří spisek B. Ježka "*Nástin röntgenometrie krystalů*" (Praha 1923), kniha profesora experimentální fyziky na pražské české univerzitě Václava Posejpalá "*Roentgenovy X paprsky*" (Praha, Jednota československých matematiků 1925) a dodnes aktuální monografie A. Kochanovské "*Zkoušení jemné struktury materiálu Röntgenovými paprsky*" (1. vydání Praha, Elektrotechnický svaz českomoravský 1941)

## MORF - A COMPUTER PROGRAM FOR PLOTTING CRYSTAL SHAPES

L. Palatinus

*Department of Geology, Faculty of Natural Sciences,  
Charles University, 128 02 Praha, Czech Republic*

In solving problems of mineralogical crystallography and related topics, there is often need for drawing a crystal shape of some sample. MORF is especially designed to make this process easy and quick. Although this is of special interest to mineralogists, it may be useful for virtually all, who come in touch with physics of solid state.

Input consists of point group, lattice parameters, and Miller's indices of crystal forms together with  $d$  – the distance of one crystal face from the centre of the crystal.

From these data the MORF program draws the crystal. It is possible to view it and make changes. This includes adding or removing some forms and changing their  $d$ . This allows drawing a crystal without knowing its  $d$ , with just inputting all  $d$  equal 1 and changing it later to appropriate values. All changes can be done graphically without inputting any numbers and are immediately shown on the screen.

During using the MORF program I realised, that with little practice and basic knowledge of morphological crystallography it is possible to plot any crystal in 10 or 20 minutes.

In nature, crystals are only rarely perfectly symmetric. Much more common is some kind of asymmetry. With MORF it is possible to change  $d$  of every face individually, and thus reach the best agreement with the intended shape. Thanks to this it is also possible to get very quickly the  $d$  ratios for all the faces of the crystal without measuring it.

Inasmuch as the MORF program can serve also for students to learn principles of morphological crystallography, it has also the facility of showing stereograms of crystal faces and all the symmetry elements for given point group.

The program is written in Turbo Pascal and works under MS-DOS or Windows operation system. It has minimal hardware requirements, although for comfortable use a computer with at least 486 processor or equivalent is recommended.

## FOURIER ANALYSIS OF A LINEAR OBJECTS

Stanislav Němeček

*Škoda Research, Ltd., Tylova 46, 316 00 Plzeň,  
Czech Republic*

### Introduction

Fourier analysis is used with advantage in many fields of science - in crystallography, spectroscopy, optics and other. An important place Fourier transform (FT) plays significant role are software programs for processing and analyses of images where it is hidden under mysterious abbreviation FT. There it serves in noise filtering, deformed pictures reconstruction [1,2], symmetry and orientation determining (for instance measurement of microcrack orientation in concrete [3]), image recognition (fingerprints recognition [4]) etc.

The principle of the method is very simple: original real image is transformed to reciprocal (Fourier) space. Required correction of the frequency spectrum is done in this space and the back (inverse) transform returns the picture into its original space. Now already with appropriate corrections. These steps can be done using the fact that the Fourier transform of our object appears in the focal plane of a lense by means of which the object is observed. So, FT-manipulation is done in the focal plane and the corrected image will be observed (photographed) in the image plane. But it is also possible to use a mathematical treatment which gives us the FT of the object under consideration by numerical operation [5,6] making use of a digitised representation of the object, obtained e.g. by a scanner.

### Abbe's theorem

Abbe's theorem speaks on a simple relation between the shape of the object and the outlook of its diffraction pattern: if the object contains straight edge, its diffraction pattern in the reciprocal space manifests stars with arms perpendicular (as it is usual in the Fourier transform) to the straight features of the object [7]. If the theorem is valid for Fraunhofer diffraction it will be valid (on certain conditions) for FT too [8].

### Texture evaluation

A typical problem encountered in microscope analysis of forged products is the determination of grain orientation or the degree of deformation (e.g., for transformer sheets...).

First of all we consider model with one grain. Grain shape is circular (spectral patterns will be central symmet-

**Fig. 1** Fourier spectrum for rectangular object. The arm of transform perpendicular to longer edge of the rectangle

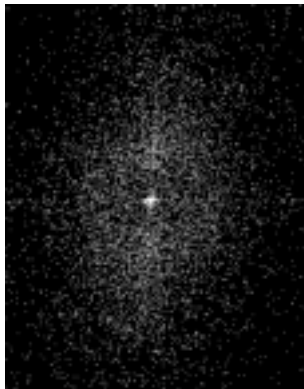


**Fig. 2** No direction is dominant in polyhedral structure and transform is roughly central symmetric; we obtain texture arrangement by deformation; deformation show itself in frequency spectrum by image elongation

ric) or better square-like. Its spectrum has two mutually perpendicular arms of equal length. By forging, the two sides of the square grain increase and the other two decrease (provided that grain's circumference is constant) - the square transforms into an oblong. The arms in the reciprocal space, which are perpendicular to longer sides of rectangle, become longer while the other two arms diminish, see fig.1.

The same situation applies for polycrystalline structures on fig.2. Starting appearance of the grains have no preferential orientation and their diffraction pattern is predominantly central symmetric. The grains start elongated by forming and, as mentioned before, shape of the diffraction pattern will be changed in a corresponding manner. Elongation of grain is due to alignment of boundaries and their subsequent stretching. FT has a preferred orientation in the direction perpendicular to material texture, exactly according to the Abbe's claim. The described procedure can make evaluation of acicular structures easier. Laborious counting of a grating intersections and determination of level orientation of system, introduced by Saltykov [9] in half of this century, is replaced by a shape characteristic of only one object - diffraction image. Appearance of the so called directional rose (number of intersections in defined direction in polar co-ordinates) is similar (by shape and contents) to Fourier spectrum. Computer aided system can proceed fully automatically.

Similar procedure can be applied to a number of other structure like: pearlitic lamellae, columnar grains in ingots, sedimentation layers or textiles, and so on.

#### Enhancing acicular features of an image

We meet oriented objects in metallography relatively often. The main axes of dendrites grow preferentially in the direction of temperature gradient or some new phases precipitate in certain directions (depending on crystallographic orientation of matrix) etc.

For quantitative evaluation, we need to separate (enhance) the oriented feature from the rest of the micrograph. In 1968, Goodman [10] described Abbe-Porters experiment from beginning of this century. By filtering of a part of frequency spectrum (in the back focal plane) the image was divided in accordance with the orientation, fig.3.

This idea serves in Widmanstätten structure evaluation on fig.4. The part of ferritic phase precipitated as needles and the rest are polyhedral grains. The dark matrix is eutectoid pearlitic phase. For quantitative measurement, we need to discriminate the oriented and the non-oriented elements. Separation according to grey level is not possible.

The needles show itself in the back focal plane by characteristic arms, fig.4. By using of a convenient filter mask we obtain after inverse transform two pictures basically - one contains only needles and the other one just the polyhedral grains of pearlit and ferrite.

#### Conclusions

The contribution presented two possibilities to use the Fourier transform in metallography: in textures evaluation and in enhancement of acicular features. Similarity of light spreading description and image processing (based on Fourier equations solving) is briefly discussed.



**Fig. 3** The Abbe-Porter experiment arrangement (a); Mesh filtered with a vertical (b) and a horizontal (c) slit-spectrum and image

Changes of the shape of Fourier spectrum as consequence of elongation of original structures are mentioned.

- [1] V. Krzyžánek: *Jemná mechanika a optika* 4 (1998) 111
- [2] D.N. Wang, S. Hovmoller: *Ultramicroscopy* 25 (1988) 303
- [3] C. Redon, L. Chermant, J.L. Chermant, M. Coster: *Acta Stereologica* 16/3 (1997) 287
- [4] D.M.Berfanger, N.George: *Applied Optics* 38/2 (1999) 357
- [5] B.E.A.Saleh, M.C.Teich: *Fundamental of Photonics*, Willey, New York 1991
- [6] J.Fiala: *Materials Structure* 3 (1996) 24
- [7] J.Komrska: *Czech Journal of Physics A27* (1977) 579
- [8] J.Komrska: *Pokroky matematiky, fyziky a astronomie* 29 (1984) 579
- [9] S.A.Saltykov: *Stereometric Metallography*, Metallurgizdat, Moscow 1958
- [10] J.W.Goodman: *Introduction to Fourier transform*, Mc Graw-Hill, San Francisco 1968

**Fig. 4** Widmanstätten structure with ferritic needles and its frequency spectrum.

## REFINEMENT OF TEMPERATURE PARAMETERS IN X-RAY POWDER DIFFRACTION

**P. Freundlich**

*Department of Materials Engineering, Faculty of Metallurgy and Materials Engineering, VŠB-TU Ostrava, 17. listopadu 15, 708 33 Ostrava-Poruba, Czech Republic*

Temperature parameters calculated from x-ray diffraction patterns of polycrystalline solids often yield too low, sometimes even negative values. Since in structure refinement the main interest is usually focused on structure parameters, the physically meaningless values of temperature parameters are usually simply ignored. Although for tens of years it has been well known that this phenomenon is caused by surface roughness of samples, no standard systematic correction has been proposed.

So far, the most rigorous treatment of the problem was proposed by Hermann and Ernrich [1] who developed a model describing the influence of rough surface on diffracted intensities and incorporated it into the Rietveld method [2]. For the description of a rough surface they used a quite complex model based on stochastic geometry requiring three independent parameters. Suortti [3] described the influence of surface inhomogeneities by only two parameters, but his model was largely empirical since no physical meaning was connected with the parameters.

Recently, a simple model of rough surface has been developed in which the thickness of the disordered surface layer is the only parameter [4]. The so-called surface roughness factor decreases intensities with decreasing diffraction angle, i.e. With increasing  $d$ . As the temperature factor decreases diffracted intensities with increasing diffraction angle, high correlation between the surface roughness parameter and the temperature parameter arises. Thus, if not treated, the surface roughness of a sample results in

too low intensities at lower scattering angles. In subsequent least squares fitting of either whole pattern profile or integrated intensities, the temperature parameter compensates this systematic error and yields incorrect values.

The correlation of these two factors has been studied in multidimensional parametrical space. While, for example, the systematic error caused by the correlation between occupancy parameters and the temperature parameter can be reduced by wide angle scans and a better experimental technique [5], the correlation between the temperature parameter and the surface roughness parameter is the result of nonorthogonality of the factors in multidimensional parametrical space and thus can not be avoided.

Simulations of diffraction patterns of simple structures have been carried out in order to show the angular dependence of the surface roughness factor and the correlation between the temperature parameter and the surface roughness parameter. The angular range of  $2\theta$  has been determined in which the influence of the surface roughness can not be neglected.

The above mentioned method allows better refinement of the mean atomic displacements from x-ray diffraction measurements on polycrystalline solids with rough surfaces and, in addition, the determination of the thickness of the disordered surface layer.

1. H. Hermann M. Ermrich, *Acta Cryst.*, **A43** (1987) 401-405.
2. W. Pitschke, N. Mattern & H. Hermann, *Mat. Sci. Forum*, bf **166-169** (1994) 103-108.
3. P. Suortti, *J. Appl. Cryst.*, **5** (1972) 325-331.
4. P. Freundlich, *Materials Structure in Chemistry, Biology, Physics and Technology*, **4** (1997) 25 (abstract in Czech).
5. E.H. Kisi, *Materials Forum*, **18** (1994) 135-153.

## STRUCTURE STUDY OF Fe/Au MULTILAYERS

**J. Lhotka, D. Rafaja, J. Vacínová, V. Valvoda**

*Faculty of Mathematics and Physics, Charles University, Ke Karlovu 5, 12116 Prague 2, Czech Republic*

We have studied the structure of Fe/Au multilayers which were prepared by diode sputtering of constituent materials on glass substrates. The following phenomena occur in the multilayer system: giant magnetoresistivity [1], enhancement of the magnetic moments [2] and magneto-optical (Kerr) rotation.

X-ray analysis was used for investigation of multilayers. Several parameters were determined from measurements done in the high angle region (HAR) by using kinematical theory: thickness of a bilayer, thickness of sublayers, average interplanar spacing, d-spacing of components, interface roughness, interlayer and intralayer disorder. Values of relative electron density of particular layers, thickness of whole layers, interface roughness were obtained from low-angle X-ray diffraction analysis (LXRD).

The thickness of Au layers was kept constant at approximately 20 Å and thickness of Fe layers was varied be-

tween 5 and 95 Å in our set of samples. Difference in the electron density in comparison with bulk values was observed. Parameters characterising disorder like interface roughness, intralayer and interlayer disorder do not change substantially with increasing thickness of particular layers.

The influence of annealing on the structure of samples has been investigated. Several samples were annealed for 60 minutes in argon atmosphere at 300 °C. The quality of multilayers decreased in general: interlayer disorder, interface roughness increases (especially the low scale interface roughness obtained from HAR increases). The extent of damage is being related to the thickness of constituent layers. Samples with thickness of iron layer  $t_{Fe}$  larger than the thickness of gold layer  $t_{Au}$  are influenced less in comparison with these with  $t_{Fe} \sim t_{Au}$ . Explanation of this effect was found in lower melting point of Au and miscibility gap in the binary phase diagram of these metals.

[1] Honda, S.; Koguma et al., *J. Appl. Phys.*, **82**: 9 (1997) 4428-4434

[2] Krishnan et al., *JMMM* **168**(1997) 15-17

## MONOCHROMATIZATION OF X-RAY RADIATION WITH PERIODIC MULTILAYERS

**J. Novák**

*Department of Solid State Physics, Faculty of Science, Masaryk University, Kotlářská 2, 611 37 Brno  
E-mail: genov@physics.muni.cz*

We have designed and built a two-mirror-monochromator in the (+,+) set-up for X-ray reflectivity measurements at the  $CuK_{\alpha}$  wavelength. The properties of the monochromatized beam have been studied and measured data have been compared to simulations. This set-up yields ten times larger angular acceptance than a usual crystal-monochromator and it transmits both lines of the  $K_{\alpha}$  doublet in the whole angular range.

We have used planar periodic multilayers  $20 \times (NiN, CN)$  with the nominal period 100 Å as the monochromator mirrors. The parameters of the multilayers, such as the multilayer period and the roughness of interfaces, have been characterized by means of specular X-ray reflectivity. The reflectivity of the first Bragg maximum has been 92 %, its angular FWHM has been about 160 arcsec for  $CuK_{\alpha 1}$ . The pair of mirrors have been adjusted to the (+,+) dispersion set-up.

The properties of the beam monochromatized by the designed monochromator have been measured by means of a single-crystal spectrometer. The X-ray source was a sealed Cu tube with a 4 mm  $\times$  0.04 mm line focus at the take-off angle of 6 deg. We have achieved the reflectivity of 80 % of the 1st Bragg peak of the monochromator for the  $CuK_{\alpha}$  lines, the FWHM being about 120 arcsec. The measure of the monochromator effectivity is the ratio  $I_{\beta}/I_{\alpha 1}$  of the intensities of the  $K_{\beta}$  and  $K_{\alpha 1}$  lines. In our arrangement we have obtained  $I_{\beta}/I_{\alpha 1}$  of about  $4 \times 10^{-4}$ . Finally, the calculations have been performed of the measured spectral den-



sity of monochromatized beam on the basis of the paraxial approximation. The simulations have fitted well the measured data, which confirms the correct adjustment of the monochromator.

## X-RAY REFLECTION ON LATERALLY STRUCTURED MULTILAYERS SIGE

**M. Meduňa<sup>1</sup>, V. Holý<sup>1</sup>, J. Kuběna<sup>1</sup>,  
J. Stangl<sup>2</sup>, G. Bauer<sup>2</sup>, J. Zhu<sup>3</sup> and  
K. Brunner<sup>3</sup>**

<sup>1</sup> *Laboratory of Thin Films and Nanostructures, Masaryk University, Brno, Czech Republic  
mjme@physics.muni.cz*

<sup>2</sup> *Institut for Semiconductor Physics, J.Kepler University, Linz, Austria*

<sup>3</sup> *Walter Schottky Institut, Technische Universität München, Germany*

We have studied the interface morphology of 20x Si<sub>0.55</sub>Ge<sub>0.45</sub>/Si strained multilayers grown by molecular beam epitaxy (MBE). Two multilayer samples grown on Si(001) have been investigated by means of x-ray specular and diffuse small angle reflection. The surfaces of both samples were intentionally misoriented with respect to (001) plane and the directions of the miscut were close to (110) and (100), respectively.

From the x-ray specular reflectivity data we determined the parameters of the multilayers, such as thicknesses of the layers and the multilayer periods. The distribution of the diffusely scattered intensity in reciprocal space is sensitive to the morphology of the interfaces in the multilayers. Very closely distributed small dots and large flat islands, formed in Stranski-Krastanow growth, were observed in AFM pictures. These structures on the sample surface give rise to lateral satellites in reciprocal space, giving information on their shapes and their in-plane arrangements. The scattering measurements were carried out in two azimuthal directions of the scattering plane (parallel and perpendicular to the surface misorientation) and the results were compared to the AFM pictures.

In our case, two kinds of lateral maxima in reciprocal space have been detected, corresponding to the small dots and large islands visible in AFM pictures. A small asymmetry in the satellite heights with respect to specular reflection is observed for both satellite types; the asymmetry corresponds to the misorientation of the surface. We also estimated the direction of the interface replication, and the correlation properties of the interfaces, that cannot be derived from AFM.

## IN SITU MECHANICAL TESTS OF MATERIALS AT HIGH-RESOLUTION NEUTRON DIFFRACTOMETERS

**D. Neov**

*Nuclear Physics Institute, Řež near Prague, 250 68 Czech Republic*

Because of relatively high penetration in most of materials neutron diffraction is eligible method of studying the evolution of the material microstructure under external loading. The neutron diffraction technique can provide information on both macro- and micro-strains [1]. The determination of macrostrains ( $\epsilon = \Delta d/d_0$ ) is based on the measurement of small angular shifts of Bragg diffraction peaks caused by small lattice-parameter variations  $\Delta d$  in a sampled volume with respect to the stress-free lattice spacing  $d_0$ . The magnitude of stress can be calculated by using appropriate elastic moduli. Investigation of microstrains is based on the analysis of the shape of broadened diffraction profiles. Of special interest are deformation tests realized *in situ* at the neutron diffractometers. In this case, the precise angular position of the profile maximum provides information on an averaged elastic strain in the sampled specimen volume whereas the width and shape of the diffraction profile is related to the evolution of the plastic deformation. The suitable instrumentation for such a kind of experiments is available in NPI Řež - two high-resolution ( $\Delta d/d \approx 2 \times 10^{-3}$ ) neutron strain scanners TKS-400 and SPN-100, equipped with a deformation rig enabling both tensile and compressive tests up to maximum loading of  $\pm 20$  kN.

Recently, much work has been done investigating various materials of technological interest, e.g. metals, composites, plasma sprayed materials and geological samples. The usefulness of this technique are illustrated by the examples of investigations of deformation properties of duplex  $\alpha/\gamma$  stainless steels. One reflection of each phase was examined - ferrite 110 and austenite 111, respectively. Evaluation of lattice strains brings information on strain partitioning between both phases. Another example of investigation of multiphase materials is Cu-based shape memory alloy (Cu-10wt.%Al-5wt.%Zn-5wt.%Mn) [2]. The shape memory effect is derived from the thermoelastic martensitic transformation in solid state induced by external mechanical or thermal loading. The analysis of recorded diffraction profiles on the  $\sigma$ - $\epsilon$  curve yielded accurate information on the: (i) evolution of the volume fractions of the transforming phases and, particularly, quantitative in-situ information on the evolution of the (ii) elastic strains and (iii) microstresses in mutually transforming austenite and martensite phases.

1. *Materials structure in Chemistry, Biology, Physics and Technology*, Vol. 4, 1997, pp.119.

2. P. Šittner and V. Novák, *Trans. of ASME, J. Eng. Mat. Tech.*, 121, (1999) 48.

## THERMAL DECOMPOSITION OF $\text{Fe}_2(\text{SO}_4)_3$ - THE DEMONSTRATION OF POLYMORPHOUS CHARACTER OF IRON (III) OXIDE

R. Zbořil<sup>1</sup>, M. Mašláň<sup>2</sup> and D. Krausová<sup>1</sup>

<sup>1</sup>Department of Inorganic and Physical Chemistry, Palacky University, Svobody 8, 77146 Olomouc, Czech Republic.

<sup>2</sup>Department of Experimental Physics, Palacky University, Svobody 26, 77146 Olomouc, Czech Republic.

The mechanism of thermal conversion of  $\text{Fe}_2(\text{SO}_4)_3$  is in principle the same both in oxidizing and inert atmosphere. At temperatures about 480°C the conversion of  $\text{Fe}_2(\text{SO}_4)_3$  crystal lattice is initiated and iron (III) oxide is formed as a solid product of this transformation. The generated  $\text{SO}_3$  undergoes a partial dissociation to  $\text{SO}_2$  and  $\text{O}_2$ . The formed  $\alpha\text{-Fe}_2\text{O}_3$ , in its nascent state, catalyzes this dissociation. The phase composition of calcination products was studied using x-ray powder diffraction and Mössbauer spectroscopy combination that appears as a powerful tool for the study of the thermally induced solid-state reactions [1-3]. In addition to the most known hexagonal alpha (hematite) modification, another infrequent modifications of  $\text{Fe}_2\text{O}_3$ , gamma, beta and epsilon, were identified in the final phase mixture.  $\gamma\text{-Fe}_2\text{O}_3$  (maghemite) - inverse spinel of cubic symmetry is the completely oxidized form of  $\text{Fe}_3\text{O}_4$  (magnetite). It also, in analogy to  $\text{Fe}_3\text{O}_4$ , contains iron in tetrahedral A and octahedral B sites, but there are vacancies (usually in octahedral positions) to compensate the increased positive charge. Thus, the stoichiometry can be indicated as  $\text{Fe}^{\text{A}}(\text{Fe}_{5/3}(\text{vac})_{1/3})^{\text{B}}\text{O}_4$ . Ordering of the vacancies leads to superstructure lines in the x-ray diffraction pattern and reduces the symmetry to tetragonal. ( $\beta\text{-Fe}_2\text{O}_3$  is a body centered cubic (bixbyite) structure with Ia3 space group and a lattice parameter  $a = 9.404 \text{ \AA}$ . 24  $\text{Fe}^{3+}$  ions in the cubic unit cell have C2 symmetry (d site) and 8 ions have C3; symmetry (b site). The Neel temperature of magnetic transition was observed between 100K and 119K. ( $\beta\text{-Fe}_2\text{O}_3$  is only a form of iron (III) oxide which is magnetically disordered at room temperature and its room temperature Mössbauer spectrum shows only the pure quadrupole splitting. The Mössbauer spectra measured below the Neel temperature contain two magnetically split subspectra with relative intensities of 3:1. This ratio corresponds to the ratio of Fe nuclei occupying the d and b sites in the cubic unit cell.

We have published previously that this spinel oxide is also one of the primary products of solid state reaction between NaCl and  $\text{Fe}_2(\text{SO}_4)_3$  as well as the product of thermal conversion of  $\text{NaFe}(\text{SO}_4)_2$  and  $\text{Na}_3\text{Fe}(\text{SO}_4)_3$  [1].  $\epsilon\text{-Fe}_2\text{O}_3$  is a orthorhombic dark brown the least known modification of iron (III) oxide. It is a noncollinear ferrimagnet with a magnetic transition at 225°C. Gamma, beta and epsilon modifications are thermally unstable and they transform into  $\alpha\text{-Fe}_2\text{O}_3$  at temperatures higher than 500°C. Thus different forms of  $\text{Fe}_2\text{O}_3$  are formed directly from ferric sulfate and thermally metastable modifications are instantaneously transformed into  $\alpha\text{-Fe}_2\text{O}_3$ . It was proved

experimentally that the calcination temperature,  $\text{Fe}_2(\text{SO}_4)_3$  particles size, modification of the initiated sulfate (rhombohedral or monoclinic) and conditions for the removal of the gaseous phases are the most important factors that influence the kinetics of the process and the percentages of the individual  $\text{Fe}_2\text{O}_3$  modifications in the thermally treated samples.

1. R. Zbořil, M. Mašláň and D. Krausová: The mechanism of  $\text{Fe}_2\text{O}_3$  formation by the solid state reaction between NaCl and  $\text{Fe}_2(\text{SO}_4)_3$ , in Mössbauer Spectroscopy in Materials Science, M. Miglierini and D. Petridis (eds.), Kluwer Academic Publishers, 49,1999.
2. R. Zbořil, M. Mašláň, D. Krausová and P. Píkal: *Hyperfine Interactions*, (1999), in print.
3. R. Zbořil, M. Mašláň, F. Grambal and D. Krausová: *Czech. J. Phys.* **47(5)**, 565 (1997).

## PHASE BEHAVIOR OF PEO/PMMA BLENDS

M. Horký<sup>1</sup>, J. Baldrian<sup>2</sup>, M. Steinhart<sup>2</sup>

<sup>2</sup>Faculty of Nuclear Sciences and Physical Engineering, Czech Technical University, V Holešovičkách 2, 180 00 Prague 8, Czech Republic, horky@troja.jffi.cvut.cz

<sup>1</sup>Institute of Macromolecular Chemistry, Academy of Sciences of the Czech Republic, Heyrovský Sq.2, 162 06 Prague, Czech Republic

Crystallization of the low-molecular PEO/PMMA blends has been intensively studied [1,2]. It has been found that in the beginning of the crystallization process the crystalline component – poly(ethylene oxide), PEO – forms lamellar structure with non-integrally folded chains (NIF). This thermodynamically unstable structure subsequently changes itself to extended and/or once-folded chains lamellae. The influence of amorphous diluent content – poly(methyl metacrylate), PMMA – to the crystallization of PEO is significant.

Up to now the studies of polymer crystallization have been focused to the crystal growth processes. Very little is known about the very beginning of the crystallization. Two different kinetic mechanisms are possible – the nucleation and the spinodal decomposition [3]. In case of the first one the crystallization starts from small nuclei, which then proceed to grow. In case of spinodal decomposition the blend components separates in the mixture so that density fluctuation occurs. After this separation normal crystallization occurs.

Presence of the PMMA slows the crystallization of PEO in the blends and makes it possible to distinguish between these two mechanisms by using simultaneous small (SAXS) and wide (WAXS) angle X-ray diffraction technique. If nucleation is the main crystallization mechanism involved both SAXS and WAXS peaks start to grow simultaneously. If the spinodal decomposition occurs, the SAXS peaks indicating density fluctuations in the mixture appears before WAXS reflection.

In several blends the crystallization was slow enough to observe SAXS peak of NIF structure growing several



seconds before WAXS. Also the electron density of the blend changes smoothly in this phase of the process. The leading process here is most probably spinodal decomposition. After short time crystalline peaks in wide angle region appear and the kinetics is changed to the growth of polymer crystals.

- [1] Baldrian J., Horký M., Vlček P., *Polymer* **40**(1999), 439  
 [2] Baldrian J., Horký M., Steinhart M., Sikora A., Amenitsch H., Bernstorff S., SPIE Proceedings in press  
 [3] Cahn J.W., *The Journal of Chem. Phys.* **42**(1965), 93  
 [4] Imai I., Kaji K., Kanaya T., Sakai Y., *Phys. Rev. B Condensed Matter.* **529**(1995), 12696  
 [5] Ryan A.J., Terrill N.J., Patrick J., Fairclough A., *Polymer Preprints* **39**(1998), 358

## STUDY OF THE MAGNETIC AND STRUCTURAL PROPERTIES OF IRON NITRIDES BY MÖSSBAUER SPECTROSCOPY

A. Kláriková<sup>1,2,3</sup>, K. Závěta<sup>1</sup>, S. Vratilav<sup>3</sup>, P. Bezdička<sup>2</sup>, I. Paseka<sup>2</sup>

<sup>1</sup> Joint Lab. for Mössbauer Spectroscopy, Faculty of Math. and Phys., Charles University, V Holešovičkách 2, 180 00 Prague 8, Czech Republic

<sup>2</sup> Institute of Inorganic Chemistry, Academy of Sciences of the Czech Republic, 250 68 Řež near Prague, Czech Republic

<sup>3</sup> Faculty of Nuclear Science and Physical Engineering, Czech Technical University of Prague, V Holešovičkách 8, 180 00 Prague 8, Czech Republic

The properties of iron nitrides may be interesting for various applications because the average magnetic moment of  $\alpha''$  Fe<sub>16</sub>N<sub>2</sub> phase seems to be higher than that of  $\alpha$  Fe. We have prepared the mixtures of the iron nitrides by nitriding iron powder in various proportions of H<sub>2</sub> and NH<sub>3</sub> at 750°C [1,2], quenching to liquid N<sub>2</sub> and annealing at 130 – 150 °C. Some of the materials were also milled in various atmospheres before final anneal. The final product of preparation contained  $\alpha$  Fe,  $\gamma$  FeN<sub>x</sub>,  $\alpha'$  FeN<sub>x</sub> and  $\alpha''$  Fe<sub>16</sub>N<sub>2</sub> and the defect phase.

The results obtained by XRD, neutron diffraction, and Mössbauer spectroscopy with the final products confirmed the presence of the desired  $\alpha''$  phase, but the quantitative data differed due to the specific features of the method employed. The effect of ball milling in a nitriding atmosphere on the details of phase composition persisted to a certain extent even after subsequent heat treatment.

The neutron diffraction experiments were performed with KSN-2 powder diffractometer installed at the 15 MW research reactor in Řež near Prague with the wavelength of the monochromatic beam 0.1362 nm, resolution  $\delta d/d = 0.006$  ( $d$  - interplanar spacing). The spectra were taken at two temperatures of 7 and 300 K in a closed-cycle helium refrigerator system model CP-62-ST/1.

The specific magnetisations were measured in a Quantum Design MPMS 5 SQUID magnetometer with powdered samples placed in gelatine ampoules at 10 and 300 K in a magnetic field produced by the superconducting solenoid with maximum  $B$  up to 5 T.

Mössbauer spectra were taken in the transmission mode with the <sup>57</sup>Co in Cr matrix as the source moving in constant-acceleration mode; most of the spectra were acquired at 300 K. The local magnetic moments were assumed to be randomly oriented as verified experimentally for several spectra with well resolved sextets.

On the one hand the average magnetic moments per Fe atom  $\mu_{Fe}$  were calculated from the measured magnetic moments of the samples with the use of the nitrogen concentration from the Kjeldahl chemical analysis and on the other hand they were also derived from the measured hyperfine fields and the concentrations of Fe in various types of sites. For the conversion of the hyperfine field to magnetic moment the coefficient of proportionality for the given phase was used as published by Coey [3]. These sets of data were in a good mutual agreement with  $\sigma$  ranging from 240 to 246 emu/g.

The two sets of magnetic moments measured by SQUID and calculated from the Mössbauer spectra were rather close to each other with a maximum difference of about 5 %.

- [1] P. Bezdička, A. Kláriková, I. Paseka, K. Závěta, *Journal of Alloys and Compounds* **274** (1998) 10-17  
 [2] I. Paseka, P. Bezdička, A. Kláriková, K. Závěta, *Journal of Alloys and Compounds* **274** (1998) 248-253  
 [3] J.M.D. Coey, *J. Appl. Phys.* **76** (1994) 6632-6636  
 [4] K.H. Jack, *Proc. R. Soc. London, Ser. A* **208** (1951) 216

## MÖSSBAUER SPECTROSCOPIC STUDY OF GARNETS FROM ALMANDINE - PYROPE GROUP

K. Černá<sup>1</sup>, M. Mašláň<sup>1</sup> and P. Martinec<sup>2</sup>

<sup>1</sup> Department of Experimental Physics, Palacky University, Faculty of Science, Svobody 26, 77146 Olomouc, Czech Republic,

<sup>2</sup> Institute of Geonics of the Academy of Sciences of the Czech Republic, Studentska I 776, 708 00 Ostrava, Czech Republic.

Garnets are orthosilicates with isolated (SiO<sub>4</sub>)<sup>4-</sup> group. Their general structural formula is X<sub>3</sub>Y<sub>2</sub>Z<sub>3</sub>O<sub>12</sub>, where X represents dodecahedral coordination of these cations: Ca<sup>2+</sup>, Fe<sup>2+</sup>, Mg<sup>2+</sup> or Mn<sup>2+</sup>. Y corresponds to octahedral positions of ions: Al<sup>3+</sup>, Cr<sup>3+</sup>, Fe<sup>3+</sup>, Ti<sup>4+</sup> or Zr<sup>4+</sup> and Z to tetrahedral positions of Si<sup>4+</sup>. In garnets, Fe<sup>3+</sup> ions are located in 16a positions of the Ia3d space group, each ion Fe<sup>3+</sup> is surrounded by six oxygen atoms. In pure almandine (Fe<sub>3</sub>Al<sub>2</sub>Si<sub>3</sub>O<sub>12</sub>) Fe<sup>2+</sup> ions are located exclusively in 24c positions of the Ia3d space group. In pure pyrope (Mg<sub>3</sub>Al<sub>2</sub>Si<sub>3</sub>O<sub>12</sub>) Mg<sup>2+</sup> substitute Fe<sup>2+</sup> ions completely. However in natural samples both Fe<sup>2+</sup> and Mg<sup>2+</sup> ions dominate in 24c positions. The influence of Fe<sup>2+</sup> and Mg<sup>2+</sup> con-



tent on hyperfine parameters (IS - isomer shift, QS - quadrupole splitting, FWHM - full width at half maximum) of the Mössbauer spectra was studied with different natural garnets of almandine-pyrope group. Electron microprobe analysis and x-ray powder diffraction [1] were used for the determination of the garnet composition. Room temperature Mössbauer spectra of seven powdered samples were collected using a Mössbauer spectrometer in constant acceleration mode with a  $^{57}\text{Co}(\text{Rh})$  source. These spectra were fitted by two doublets.

The most intensive doublet with  $\text{IS}_{\text{Fe}} 1.28 \div 1.30$  ms and  $\text{QS}=3.47 \div 3.58$  mm/s corresponds to  $\text{Fe}^{2+}$  in the X dodecahedral position of the garnet structure. Second doublet with  $\text{IS}_{\text{Fe}} 0.33 \div 0.34$  mm/s and  $\text{QS}=0.31 \div 0.59$  mm/s originates from  $\text{Fe}^{3+}$  in the Y octahedral position. The FWHM of spectral lines of  $\text{Fe}^{2+}$  doublets are the same for samples with very low  $\text{Mg}^{2+}$  content (the structure near pure almandine). An asymmetry of the FWHM of spectral lines increases with  $\text{Mg}^{2+}$  content. Our experimental results show that the direct correlation between the  $\text{Mg}^{2+}$  content and the asymmetry of spectral lines FWHM exists. This correlation allows to select the investigating samples within the framework of almandine-pyrope group. The influence of  $\text{Mg}^{2+}$  content on other hyperfine parameters of Mössbauer spectrum (IS, QS) was not found.

[1] M. Chmielová, P. Martinec, Z. Weiss:

Almandine-pyrope-grossular garnets: a method for estimating their composition using X-ray powder diffraction patterns, *Eur. J. Mineral.* **9**, 403-409 (1997).

Full paper is to be published in *Mater. Struct.* **V. 7**, n. 1

## CHEMICAL COMPOSITION AND THE CRYSTAL STRUCTURE OF CASSITERITE

M. Klementová<sup>1</sup>

Department of Geochemistry, Mineralogy and Mineral Resources, Faculty of Science, Charles University, 128 43 Praha, Czech Republic

Cassiterite belongs to the rutile structural group whose members crystallize in space group  $P4_2/mnm$ . Cell parameters of synthetic  $\text{SnO}_2$  are:

$a = 4.7358 \text{ \AA}$ ,  $c = 3.1851 \text{ \AA}$  at  $295^\circ\text{K}$

$a = 4.7391 \text{ \AA}$ ,  $c = 3.1869 \text{ \AA}$  at  $470^\circ\text{K}$

$a = 4.7421 \text{ \AA}$ ,  $c = 3.1901 \text{ \AA}$  at  $615^\circ\text{K}$

$a = 4.7456 \text{ \AA}$ ,  $c = 3.1930 \text{ \AA}$  at  $770^\circ\text{K}$

$a = 4.7509 \text{ \AA}$ ,  $c = 3.1965 \text{ \AA}$  at  $930^\circ\text{K}$

$a = 4.7552 \text{ \AA}$ ,  $c = 3.1992 \text{ \AA}$  at  $1100^\circ\text{K}$ .

Natural cassiterites have smaller cell dimensions than the synthetic ones. According to the investigation of 35 specimens from different types of Sn-deposits in Australia, unit-cell parameters of natural cassiterite fall between  $a = 4.72824 - 4.73976 \text{ \AA}$ ,  $c = 3.18084 - 3.18755 \text{ \AA}$ .

The likely explanation of the differences is the non-stoichiometry of natural cassiterites. Their composition does not reach the ideal 78.6% of Sn. Significant contents (up to several %) of Fe, Mn, Nb, Ta, W and Ti are nearly always present. All of these elements can easily enter the structure of cassiterite substituting Sn:  $\text{Sn}^{4+} \leftrightarrow \text{Ti}^{4+}$ , 3

$\text{Sn}^{4+} \leftrightarrow 2\text{Fe}^{3+} + \text{W}^{6+}$ ,  $3 \text{Sn}^{4+} \leftrightarrow 2 (\text{Ta}, \text{Nb})^{5+} + (\text{Fe}, \text{Mn})^{2+}$ . Owing to their small radii (smaller than Sn), their substitution would tend to shrink the unit cell.

## CRYSTALLIZATION AND PRELIMINARY X-RAY DATA FROM HALOALKANE DEHALOGENASE LINB - AN ENZYME FOR $\gamma$ -HEXACHLOROCYCLOHEXANE DEGRADATION IN *Sphingomonas paucimobilis* UT26

Ivana Smatanová<sup>1</sup>, Yuji Nagata<sup>2</sup>, L. Anders Svensson<sup>3</sup>, Masamichi Takagi<sup>2</sup> and Jaromír Marek<sup>1</sup>

<sup>1</sup>Laboratory of Biomolecular Structure and Dynamics & Department of Inorganic Chemistry, Faculty of Science, Masaryk University, Kotlářská 2, CZ 611 37 Brno, Czech Republic,

<sup>2</sup>Department of Biotechnology, The University of Tokyo, Yayoi, Bunkyo-ku, Tokio 113-8657, Japan,

<sup>3</sup>Department of Molecular Biophysics, Center for Chemistry and Chemical Engineering, Lund University, S-221 00 Lund, Sweden.

The enzyme haloalkane hydrolytic dehalogenase LinB from *Sphingomonas paucimobilis* UT26 releasing chloride or bromide anion from *n*-halogenated alkanes has a broad range of substrate specificity catalyses. This enzyme was crystallized by using the hanging-drop vapor-diffusion method at 278 K. The best crystals were obtained by micro-seeding and a precipitant containing 18-20 % (w/v) PEG6000, 0.2M Ca acetate and 0.1M Tris-HCl, pH 8.9. The crystals belong to the orthorhombic space group  $P2_12_12$  with unit-cell parameters  $a=50.29$ ,  $b=71.70$ ,  $c=72.73 \text{ \AA}$  diffracted to at least  $1.60 \text{ \AA}$  [Crystallographic Beamline BL711 at the MAX-II synchrotron in Lund (Sweden) using Mar345 image plate detector] at cryogenic (100 K) conditions.

### Crystallization Experiment

Haloalkane dehalogenase LinB from *Sphingomonas paucimobilis* UT26 was overproduced in *E. coli*, purified to homogeneity, and concentrated to 2.0 mg/ml in 20mM potassium phosphate, pH 6.8, 1 mM 2-mercaptoethanol buffer by Yuji Nagata (Nagata *et al.*, 1997). The protein solution was exchanged by the purification buffer [10 mM Tris-HCl, pH=7.5] and the enzyme was concentrated to 14.4 mg/ml with Beckmann Avanti Centrifuge J-30I at 5000 g. All crystallization experiments were performed at 278 K by the hanging-drop variant of the vapor-diffusion method in VDX plates (Hampton Research). Drops contained 4  $\mu\text{l}$  of the respective reservoir solution and 4  $\mu\text{l}$  of the enzyme.

The initial crystallization trials were carried out using the reservoirs consisted of 1 ml each of Hampton Research Crystal Screen (Jancarik & Kim, 1991) and Crystal Screen II (Cudney *et al.*, 1994). Formation of crystalline material was observed in Jancarik's conditions 36 [8% (w/v) polyethylene glycol  $M_r$  8000 (PEG 8000), 0.1 M Tris-HCl,



pH 8.5] and 46 [18% (w/v) PEG 8000, 0.1 M Sodium cacodylate, pH 6.5, 0.2 M Ca acetate] after one week. pH, PEG and Ca acetate concentrations were optimized and very thin two dimensional crystals LinB from heavy precipitated protein were grown in solution containing 17-19% (w/v) PEG 6000, 0.2M Ca acetate and 0.1M Tris-HCl, pH 8.8-9.0 during two even three weeks. These crystals were used for microseeding and macroseeding (Stura & Wilson, 1992). The best result was obtained from the microseeding experiment as follows. The droplets containing 10  $\mu$ l of enzyme and 10 $\mu$ l reservoir solution [18% (w/v) PEG 6000, 0.2M Ca acetate and 0.1M Tris-HCL, pH 8.9] were equilibrated 24 hours after which they were centrifuged at 10000 g to remove precipitate. A seed stock was produced by washing five previously prepared small crystals in 100  $\mu$ l of their precipitant solution. Subsequently the crystals were crushed and the stock was homogenized. Crystallization was initiated by mixing droplets composed from 4.2 $\mu$ l supernatant and 1.4 $\mu$ l seed stock. Large plates of LinB grew to an average size of about 0.8 x 0.4 x 0.02-0.04 mm after two to three weeks.

### Crystal Characterization

A single crystal of LinB with dimensions 0.6 x 0.35 x 0.03 mm was immersed in cryoprotectant [20% (w/v) PEG 6000, 10% (w/v) sucrose, 10% (v/v) PEG 400] for a few seconds and rapidly exposed to a cold nitrogen stream (Oxford Cryostream Cooler). X-ray data were collected at the crystallographic beamline BL711, MAX-II synchrotron, Lund (Sweden) at 100.0 K using mar345 image plate detector. Wavelength used was  $\lambda = 0.9420$  Å. All data were processed and merged using the XDS system (Kabsch, 1993).

The crystal of LinB from *Sphingomonas paucimobilis* UT26 diffracted to 1.60 Å. The crystal belongs to the orthorhombic space group P2<sub>1</sub>2<sub>1</sub>2 with unit-cell parameters a=50.29, b=71.70, c=72.73 Å. The asymmetric unit containing one molecule of the enzyme gives a  $V_m$  of 2.1 Å<sup>3</sup>Da<sup>-1</sup>. The solvent content is then approximately 42%.

### Acknowledgements

*This work was supported in part by a grant-in-aid from the Ministry of Education, Science, and Culture of Japan (to YN and MT) and by grant VS96095 from Department of Education of the Czech Republic (to IS and JM). JM thanks Svenska Institutet for his scholarship.*

1. Cudney, B., Patel, S., Weisgraber, K., Newhouse, Y. & McPherson, A. (1994). *Acta Cryst.* **D50**, 414-423.
2. Jancarik, J. & Kim, S.-H. (1991). *J. Appl. Cryst.* **24**, 409-411.
3. Kabsch, W. (1993). *J. Appl. Cryst.* **26**, 795-800.
4. Nagata, Y., Miyauchi, K., Damborský, J., Manová, K., Ansorgová, A. & Takagi, M. (1997). *Appl. Env. Microbiol.* **63**, 3707-3710.
5. Stura, E. A. & Wilson, I. A. (1992). *Crystallization of Nucleic Acids and Proteins. A practical Approach*, edited by A. Ducruix and R. Giegé, pp. 99-125. Oxford : Oxford University Press.

## OLIGONUCLEOTIDE D(GCGAAGC) CREATED SHORT HAIRPIN IN SOLUTION: CRYSTALLIZATION, FOR X-RAY DIFFRACTION STUDIES

J. Vévodová and J. Marek

*Laboratory of Biomolecular Structure and Dynamics, Masaryk University Brno, Czech Republic*

Studied oligonucleotide having a sequence d(GCGAAGC) has been described as an extraordinary stable hairpin structure in solution [1].

Melting point of the structure consisting of the two hydrogen bonding G-C base pairs and of the GAA loop is as high as 76.5°C, the highly stacked structure shows strong resistance against nucleases contained in E. Coli extracts as well [1].

Crystallization trials were conducted using the Hampton Nucleic Acid Mini Screen [2]. The diffracting crystals were obtained at 4°C by the hanging drop vapor-diffusion technique from 10% MPD, 20 mM Cobalt Hexamine, 12 mM NaCl, 80 mM KCl in 40 mM Sodium Cacodylate-HCl pH 5.5 solution with 35% v/v MPD as the dehydratant.

The crystals diffracting at BL711 station in MAXII synchrotron in Lund to resolution below 2 Å (at 100 K) belong to tetragonal space group P43212 (or P41212) with unit cell parameters a = 48.28, c = 63.36 Å. Structure determination is currently in progress.

*The work was supported by grant No vS96095 of the Dept. of Education of the Czech Republic and by travelling grant (JM) of Svenska Institutet.*

1. I. Hirao, G. Kawai, S. Yoshizawa, Y. Nishimura, Y. Ishido, K. Watanabe, L. K. Miura (1994), *Nucleic Acids Research*, **22**, 576-582.
2. I. Berger, Ch. Kang, N. Sinha, M. Wolters & A. Rich (1996), *Acta Cryst.*, **D52**, 465-468.

## ANTI - HIV PROTEINASE MONOCLONAL ANTIBODY F11.2.32 THAT INHIBITS ENZYME ACTIVITY

R. Štouračová<sup>1</sup>, J. Lescar<sup>3</sup>, Jiří Brynda<sup>1</sup>, M.-M. Riottot<sup>2</sup>, V. Chitarra<sup>2</sup>, M. Fábry<sup>1</sup>, M. Hořejší<sup>1</sup>, P. Řezáčová<sup>1</sup>, G. Bentley<sup>2</sup> and J. Sedláček<sup>1</sup>

*1 Department of Gene Manipulation, Institute of Molecular Genetics, Academy of Sciences of the Czech Republic, 166 42 Prague, Czech Republic*

*2 Unité d'Immunologie Structurale, Institut Pasteur, Paris, France*

*3 High brilliance Beamline ID2, ESRF Grenoble*

The hybridoma that produce inhibitory monoclonal antibody (mAb) termed F11.2.32 originate from mice immunized with recombinant proteinase of HIV-1. This mAb belongs to IgG1 isotype, and its binding and inhibitory

properties are also preserved in the corresponding Fab fragment.

HIV-1 protease is a homodimeric enzyme belonging to the family of aspartic proteinases. The monomer comprises 99 amino acid residues containing a triplet AspThrGly which is located near the dimer interface. Thus, in the functional homodimer the two amino acid triplets are adjacent to each other, forming a pepsin-like catalytic site at the bottom of a hydrophobic cavity. The catalytic site is covered by two flap regions, one contributed by each subunit, which undergo substantial movement during binding the substrate.

Peptide segments 10-11 residues long, and spanning the whole HIV-1 protease sequence, were tested previously for their ability to inhibit the binding of IgG F11.2.32 to HIV-1 protease. F11.2.32 mAb has been found to be reactive to peptide MSLPGRWKPKM (positions 36-46) of HIV-1 PR. The F11.2.32 epitope relates to flap region of the enzyme. This region is involved in the substrate binding and undergoes a substantial steric transition in each turn of the catalytic cycle. To our knowledge, neither flap-reactive mAbs, nor flap-targeted inhibitors have been described up to now. The inhibitory effects found for mAb F11.2.32 remain compatible with several candidate mechanisms (e.g. interference with the flap movement, indirect distortion of the active site, dissociation of protomers).

"Titration" experiment with the flap-specific Fab F11.2.32 was carried out in analogy with conventional (low molecular weight) inhibitors, but at conditions favorable for antibody binding. The  $K_{inh}$  is  $35 \pm 2.4$  nM, whereas  $K_d = 4.8$  nM was measured by surface plasmon resonance using the BIAcore system (Pharmacia Biosensor).

Crystallographic studies were successfully concluded with Fab F11.2.32 in free state and complexed with the proteinase epitope peptides (Lescar et al., *Prot. Sci.* 5: 997, 1996; Lescar et al., *J. Mol. Biol.*, 267:1207-1222, 1997). Crystallographic data from measurements on crystals of Fab F11.2.32, Fab F11.2.32-(peptide 36-46) and Fab F11.2.32-(peptide 36-57): Specific clues for structural basis of the inhibition are provided, namely with the crystal structure of complex Fab F11.2.32 : peptide 36-46. The refined model of the complex reveals ten well-ordered residues of the peptide (P36-P45) bound in a hydrophobic cavity at the center of the antigen binding site. The peptide adopts a hairpin-like structure in which residues P38-42 form a type II  $\beta$ -turn conformation. An intermolecular antiparallel  $\beta$ -sheet is formed between the peptide and CDR3-H loop of the antibody, additional polar interactions occur between main chain atoms of the peptide and hydroxyl groups from tyrosine residues protruding from CDR1-L and CDR3-H. Three water molecules, located at the antigen-antibody interface, mediate polar interactions between the peptide and the most buried hypervariable loops CDR1-L and CDR3-H. A comparison between the free and complexed Fab fragments shows that significant conformational changes occur in the long hypervariable regions, CDR1-L and CDR3-H, upon binding the peptide. The conformation of the bound peptide, which shows no overall structural similarity to the corresponding segment in HIV-1 protease, suggests that F11.2.32 might inhibit proteolysis by distorting the native structure of the enzyme.

The tested mAb is meant to serve as „lead compound“ for constructing alternative (non-active-site) inhibitors of lower molecular weight. Several aspects of our findings are encouraging: The observed inhibition is excellent, approach to its structural basis seems to be open in principle, and situation with the flap-specific mAb F11.2.32 is greatly simplified due to predominant involvement of a single CDR in the complex formation. Even here, however, the development of mAb mimetics has proved to be far from trivial, since a simple peptide version (or cyclic peptide version) of CDR3-H does not display any inhibitory effects. The main advantage of possible potent non-active site inhibitors could be seen in different mechanisms of development of resistance to them.

---

## RECOMBINANT SCFV FRAGMENT OF AN ANTI - HIV PROTEASE ANTIBODY: CLONING, EXPRESSION, PURIFICATION AND CRYSTALLIZATION OF A COMPLEX WITH AN EPITOPE PEPTIDE.

**Pavlna Řezáčová, Jiří Brynda, Milan Fábry, Magda Hořejší, Renata Štouračová and Juraj Sedláček**

*Department of Gene Manipulation, Institute of Molecular Genetics, Academy of Sciences of the Czech Republic, Prague, Czech Republic*

The HIV protease (HIV PR) is a homodimeric enzyme belonging to the family of aspartic proteases. This enzyme plays an essential role in proper virion assembly and maturation during the HIV life cycle and is thus one of the most attractive targets for antiviral drug design [1]. Some specific substrate-based inhibitors of HIV PR are currently used as therapeutic agents in AIDS treatment but there is a problem in rapid development of drug resistance [2]. Design of alternative non-active site HIV PR inhibitors directed to other functionally important parts of the enzyme is thus necessary.

Monoclonal antibody designated 1696 have been raised against HIV-1 protease; the recognised epitope is the N-terminus (residues 1 – 8) of each subunit of both the HIV-1 and HIV-2 proteases. The antibody inhibits catalytic activity of HIV PR probably by destabilising the dimeric form required for the enzymatic activity. We have recently described the three-dimensional structure of 1696 Fab fragment in its free form [3].

In the present work we have prepared recombinant single-chain Fv fragment (scFv) of 1696 antibody as well as its complex with synthetic epitope peptide PQFSLWKR (corresponding to the N-terminus of the HIV-2 protease).

Coding sequences for light and heavy variable chains were obtained from hybridoma 1696 cells by reverse transcription of total mRNA and PCR amplification of the resultant cDNA, using appropriate pairs of primers. The scFv 1696 fragment was assembled from L and H variable domains linked by a flexible linker (Gly<sub>4</sub>Ser)<sub>3</sub>. The protein scFv 1696 was expressed from a T7 promoter driven expression plasmid in *E. coli*. A procedure adapted



from Kurucz *et al.*, 1995 [4] was used to recover a correctly refolded protein from inclusion bodies.

A purification procedure comprising three chromatography steps yielded scFv 1696 in the purity necessary for crystallization trials.

The complex was prepared by mixing scFv1696 with an excess of the epitope peptide corresponding to the N-terminus of HIV-2 PR (PQFSLWKR). Monomeric and dimeric forms of the complex were separated by FPLC on a Mono-Q column. In contrast to free scFv 1696 these forms are stable and do not interchange.

In a series of crystallization trials crystals of the complex have been obtained.

For crystallization trials by vapour diffusion method (hanging drop) only monomeric complex of the scFv1696 with epitope peptide was used. Crystals grew spontaneously at 25°C in ammonium sulfate (concentrations: 1.8 - 2.0 M) at pH 4.6. These crystals were very sensitive and flaws on their surface appeared in few days. However, this spontaneous crystallization could not be reproduced with a new batch of the complex, therefore, a streak seeding technique was applied and single crystals of size up to 0.3 x 0.3 x 0.2 mm were obtained.

Solving of 3D structure of the scFv 1696 - epitope peptide complex is expected to lead to antibody- structure-based design of a new class of HIV protease non-active site inhibitors, possibly of different HIV resistance characteristics.

1. R.A. Katz & A. M. Skalka, *Ann. Rev. Biochem.*, **63** (1994) 133-173
2. T. Ridky & J. Leiss, *J.Biol.Chem.*, **270** (1995) 29621-29623
3. J. Lescar, J. Brynda, P. Řezáčová, R. Štouračová, M. Riottot, V. Chitarra, M. Fábry, M. Hořejší, J. Sedláček & G. Bentley, submitted to *Prot. Sci.*
4. I. Kurutz, J. A. Titus, C. R. Jost & D. M. Segal, *Molecular Immunology* **32** (1995) 1443-1452

## POSTERY

### CRYSTALLIZATION AND PRELIMINARY DIFFRACTION STUDY OF HIV-1 PROTEASE COMPLEXED WITH HYDROXYETHYLAMINE INHIBITOR SI

E. Buchteřová<sup>1</sup>, J. Hašek<sup>2</sup>, J. Dohnálek<sup>2</sup>, J. Brynda<sup>3</sup>, J. Sedláček<sup>3</sup>, M. Hradílek<sup>4</sup>, J. Konvalinka<sup>4</sup>, E. Tykarská<sup>5</sup>, M. Jaskolski<sup>5,6</sup> and L. Olivi<sup>1</sup>

<sup>1</sup>Department of X-ray diffraction, Sincrotrone Trieste, Strada Statale per Basovizza, 34012 Trieste, Italy

<sup>2</sup>Institute of Macromolecular Chemistry ASCR, Heyrovského nam. 2, 16206 Praha, Czech Republic

<sup>3</sup>Institute of Molecular Genetics ASCR, Flemingovo nam. 2, 16637 Praha, Czech Republic

<sup>4</sup>Institute of Organic Chemistry and Biochemistry ASCR, Flemingovo nam. 2, 16637 Praha, Czech Republic

<sup>5</sup>Department of Crystallography, A. Mickiewicz Univ., Poznan, Poland

<sup>6</sup>Center for Biocrystallographic Research, Institute of Bioorganic Chemistry, Polish Academy of Sciences, Noskowskiego 12/14, 61704 Poznan, Poland

The HIV-1 protease is essential for replication of infective virus HIV, and therefore is an attractive target for the design of specific inhibitors. In search for new inhibitors substantial effort is placed on understanding the nature of the inhibitor binding modes in the active site, using X-ray diffraction on crystals as the primary source of structural information. Here we report crystallization of HIV-1 protease complexed with a four amino acid pseudopeptidic inhibitor, where the scissile peptide bond is replaced by hydroxyethylamine isostere. This inhibitor, Boc-Phe-[(S)-CH(OH)CH<sub>2</sub>NH]Phe-Ile-Phe-NH<sub>2</sub>, is assigned here SI.

First crystallization trials were based on crystallization studies performed with complex of HIV-1 PR with inhibitors SE, RE, RQ. These inhibitors differ from SI only in the amino acid at P2' position, carrying Glu or Gln instead of Ile, and in configuration at C4, an hydroxyl bearing carbon of the pseudopeptidic bond. Hanging drop vapor diffusion technique has been used in all experiments. In the case of Glu/Gln containing inhibitors protein - inhibitor mixture of 3 mg/ml HIV PR, 0.544 mM inhibitor (four-fold molar excess over protease) in 50 mM sodium acetate pH 5.6, 1 mM EDTA, 0.05% -mercaptoethanol, 5% DMSO was used. The optimal crystallization conditions found for these crystals are: 1M NH<sub>4</sub>H<sub>2</sub>PO<sub>4</sub>, 100 mM sodium citrate, pH 4.5, temperature 6 - 8°C [1].

In contrast to Glu/Gln containing inhibitors, SI inhibitor addition caused protein precipitation even without presence of salt precipitant. Probable reason is higher hydrophobicity of SI inhibitor. Addition of ammonium phosphate at conditions described above produced no crystal growth and no additional precipitation. Crystals of max.